ACS APPLIED NANO MATERIALS
Cite This: ACS Appl. Nano Mater. 2018, 1, 2503−2508
Letter
www.acsanm.org

Increasing Exfoliation Yield in the Synthesis of MoS_2 Quantum Dots for Optoelectronic and Other Applications through a Continuous Multicycle Acoustomicrofluidic Approach

Susan Marqus,[†] Heba Ahmed,[†] Mustafa Ahmed,[†] Chenglong Xu,[‡] Amgad R. Rezk,[†] and Leslie Y. Yeo*[,†]

[†]School of Engineering and [‡]MicroNano Research Facility (MNRF), RMIT University, Melbourne, Victoria 3000, Australia

Supporting Information

ABSTRACT: We show that the synthesis yields of transition-metal dichalcogenide (TMD) quantum dots (QDs)—in particular, that of molybdenum disulfide (MoS_2)—can be improved through a miniaturized continuous multicycle microfluidic process. The process exploits the unique piezoelectricity of two-dimensional (2D) TMDs by employing the strong electromechanical coupling inherent in a novel acoustomicrofluidic nebulization process to delaminate and laterally cleave the bulk TMD material into QDs. In particular, we show that by carrying out the process in a closed system the nebulized aerosols containing the exfoliated QDs recondense and are repeatedly renebulized. With each successive nebulization−condensation−renebulization cycle, the QDs are progressively thinned and become increasingly uniform in their lateral dimension. Over just four 10 min cycles, the yield of predominantly single-layer QDs with a mean lateral dimension of 8.25 ± 4 nm is 10.7 ± 2% with a single chipscale device, which is considerably higher than the typical 2−3% yields obtained with conventional synthesis methods. Given the simplicity, low cost, and miniaturizability of the technology, the process can be easily parallelized for high production throughput commensurate with industrial-scale synthesis for a wide range of applications across optoelectronics, photocatalysis, energy storage, photonics, and biosensing, among others.

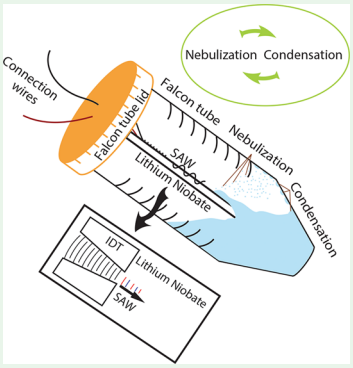

KEYWORDS: *transition-metal dichalcogenides, acoustic wave, microfluidics, quantum dots, exfoliation, piezoelectricity*

When confined to two dimensions, transition-metal dichalcogenides (TMDs) of the form MX_2 {M being the transition metal [e.g., molybdenum (Mo) or tungsten (W)] and X the chalcogen [e.g., sulfur (S) or selenium (Se)]} have been observed to possess high carrier mobility, large optical absorption, and superior mechanical strength and flexibility similar to graphene.[1] Unlike graphene, however, TMDs are semiconducting, possessing an indirect band gap when in the bulk three-dimensional (3D) state that transitions to a direct band gap when they are exfoliated into two-dimensional (2D) form and quantum dots (QDs),[2,3] thus making them ideal for use in optoelectronics[4] and as transistors,[5] among others. TMD QDs, in particular, have also found extensive applications in bioimaging,[6] detection,[7,8] and catalysis.[9]

The strong interlayer bonding between the horizontal planes that make up the TMDs, however, imposes particular challenges for exfoliating the material from its three-dimensional (3D) bulk state into QDs. In addition, the strong covalent bonding between the transition-metal and chalcogen atoms that comprise each plane makes them difficult to break laterally, particularly if uniformity in their sizes is desired. Current production techniques for MoS_2 QDs include bottom-up approaches such as hydrothermal[10] and electrochemical[11] synthesis methods or top-down approaches such as mechanical (e.g., sonication)[9] and chemical exfoliation[12] or a combination of these methods.[13] Bottom-up approaches, however, suffer from low yield (typically 2−3%) and long processing times.[14] Conventional top-down approaches are also typically slow, requiring many hours, involve the use of harsh chemicals and conditions, and often result in low yields and broad size distributions. For example, intercalating agents or solvents are commonly used together with ultrasonication under atmospheric pressure and high temperatures (≈200 °C) for 24 h;[13] in some cases, these processes involve an additional step of mechanically grinding the bulk material prior to sonication.[15] Despite these lengthy procedures, the yield remains poor, typically below 5%,[16] and small amounts of the intercalating agents or solvents are often trapped in the material because they are hard to remove, therefore leading to contamination and poor crystal quality.[12] A lone exception has been reported in the literature, in which significantly higher MoS_2 QD yields (9.65%) were obtained.[17] This method, nevertheless, still suffers from long processing times given the necessity for ultrasonicating the feedstock bulk MoS_2 solution for 20 h. This is compounded by the difficulty in removing the intercalating agent (H_2SO_4) used.

As such, a fast, cost-effective, and simple (e.g., one-step) yet efficient technique for high yield production of MoS_2 QDs with uniform sizes and thicknesses remains a challenge. In this work,

Received: April 4, 2018
Accepted: June 1, 2018
Published: June 1, 2018

DOI: 10.1021/acsanm.8b00559
ACS Appl. Nano Mater. 2018, 1, 2503−2508

we capitalize on a recently discovered acoustomicrofluidic nebulization process that exploits the unique piezoelectricity of TMDs[18] to mechanically delaminate bulk MoS_2 into intermediate 100-nm-thick flakes, which are then immediately cleaved by the electric field into monolayer and few-layer nanosheets for the rapid synthesis of MoS_2 QDs with high yields but without the need for intercalating agents.[19] We show here that cycling this process such that the nebulized feedstock condenses and is renebulized again continuously not only increases the uniformity in the thickness and lateral size of the QDs produced but also significantly increases the yield from 2%[19] to over 10% in just 40 min. Moreover, unlike conventional exfoliation using a probe sonicator,[9] the entire setup is miniaturized within a Falcon tube, which is compatible with downstream processes for further immediate processing and also scalable for high throughput through the use of a large number of devices in parallel.

Nanometer-amplitude electromechanical-wave (surface acoustic wave, or SAW[20]) devices of 30 MHz are fabricated by sputter-coating (SPI-Module Sputter Coater; Structure Probe Inc., West Chester, PA) interdigital transducers (IDTs) comprising a 10 nm chromium adhesion layer and a 500 nm aluminum film onto a piezoelectric 127.68° *Y*-rotated *X*-propagating lithium niobate substrate (Roditi Ltd., London, U.K.) with the aid of standard photolithography; the gap and width of the IDT fingers correspond to the SAW wavelength λ, which is related to its frequency f through the wave propagation speed in the substrate, i.e., $\lambda = c/f$. The SAW can then be generated by applying a sinusoidal electrical field to the IDTs using a radio-frequency signal generator (SML01; Rhode & Schwarz, North Ryde, New South Wales, Australia) and an amplifier (LYZ-22+, Mini Circuits, Brooklyn, NY) and propagates along the substrate as a Rayleigh wave.

The SAW devices were first cleaned with acetone and isopropyl alcohol (Sigma-Aldrich Pty. Ltd., Castle-Hill, New South Wales, Australia) prior to use. A device is then carefully mounted within a 15 mL Falcon tube (Sigma-Aldrich Pty. Ltd., Castle-Hill, New South Wales, Australia) prefilled with a 3 mL liquid suspension of bulk MoS_2, prepared by dissolving 50 mg of bulk MoS_2 powder ($\lesssim 4\ \mu$m lateral dimension, 99.9% purity; US Research Nanomaterials Inc., Houston, TX) in a 10 mL equipart mixture of absolute ethanol (Sigma-Aldrich Pty. Ltd., Castle-Hill, New South Wales, Australia) and deionized water (Milli-Q, Merck Millipore, Bayswater, Victoria, Australia), such that it is slightly submerged in the liquid to a depth of approximately 10 mm, as illustrated in Figure 1. A small hole was made on the lid of the Falcon tube to allow through passage of the electrical wires to connect the signal generator and amplifier to the device within the tube with the aid of two alligator clips (26 mm; Jaycar Electronics, Rydalmere, New South Wales, Australia). The lid was subsequently covered with Parafilm (Bemis Company Inc., Neenah, WI) to prevent material loss from the Falcon tube.

Upon excitation of the IDTs with a 30 V_{rms} electrical signal at its resonant frequency (30 MHz), the SAW not only generates strong acoustic streaming (i.e., recirculation) in the liquid, which has been employed elsewhere for a myriad of microfluidic applications,[21−24] but also nebulization of the liquid into micron-dimension aerosol droplets.[25] It is the unprecedented acceleration along the SAW substrate, on the order 10^8 m/s^2, which gives rise to the strong shear and compression forces accompanying the acoustic streaming and nebulization, that is responsible for the mechanical delamination of the bulk 3D MoS_2 into intermediate 100-nm-dimension flakes. Subsequently, the inherent electric field of the SAW acts to further cleave the piezoelectric flakes into few-layer sheets with ∼30 nm lateral dimensions commensurate with the MoS_2 crystal domain sizes.[19] In contrast to the single nebulization step in ref 19, however, the nebulized droplets containing the exfoliated MoS_2 sheets in the present setup condense back onto the feedstock in the closed confinement of the Falcon tube and are continuously and successively renebulized to progressively break them into smaller, thinner, and more uniform QDs. In this study, we examine the nebulization−condensation−renebulization duration in terms of 10 min cycles at a constant nebulization rate of approximately 0.29 mL/min to determine its effect on the QD size distribution and yield.

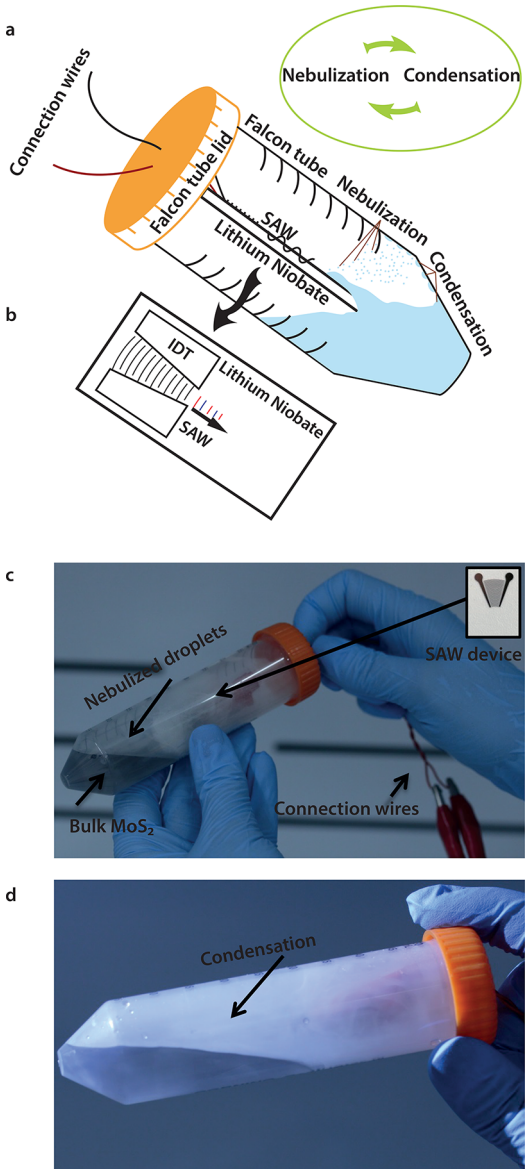

Figure 1. (a and b) Schematic depiction and (c and d) images of the experimental setup used for continuous SAW nebulization, condensation, and renebulization of a MoS_2 suspension for the synthesis of QDs. The SAW device, illustrated in part b and mounted within the Falcon tube, is shown in the inset of part c.

Following exfoliation over a specified number of these cycles, the suspension is then centrifuged at 5000 rpm for 15 min to collect the synthesized QDs without further treatment for

DOI: 10.1021/acsanm.8b00559
ACS Appl. Nano Mater. 2018, 1, 2503−2508

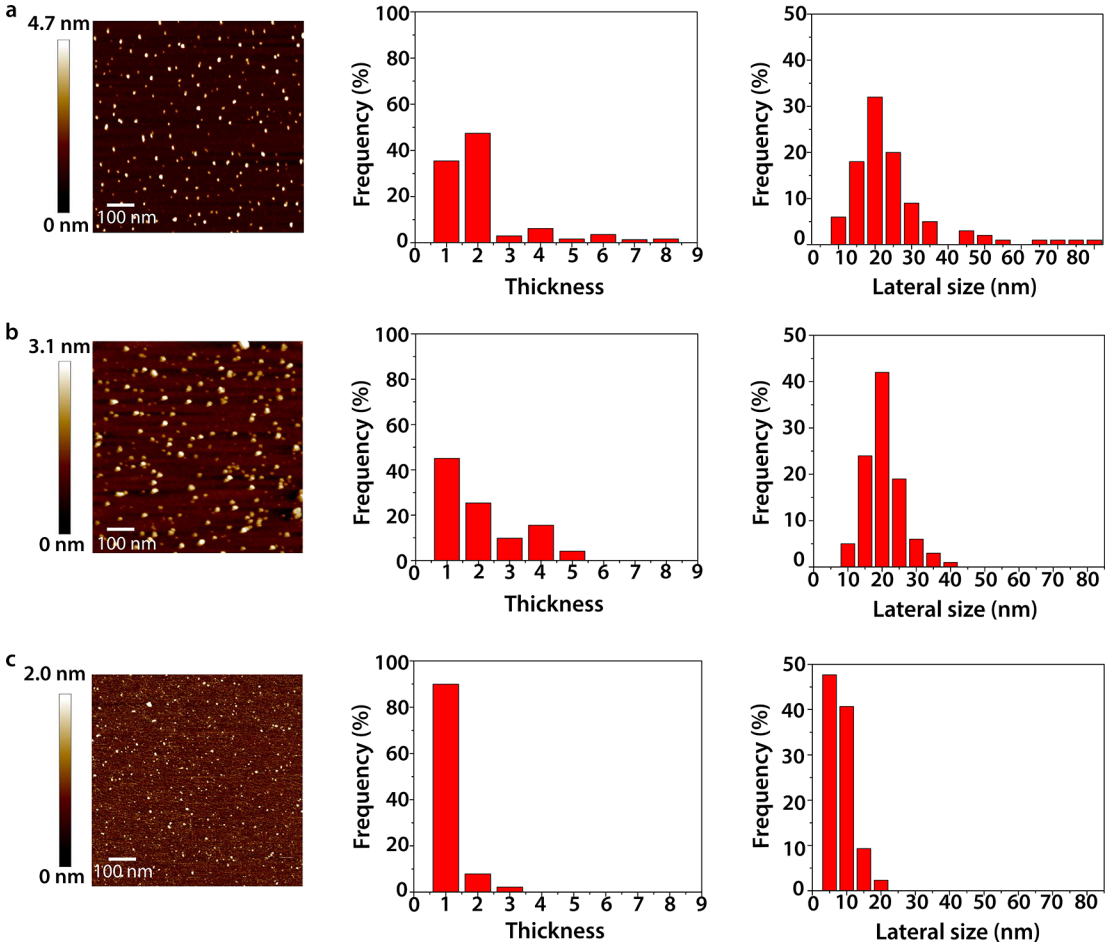

Figure 2. AFM scans (left column), number of layers (center column), and lateral sizes (right column) of the MoS_2 QDs synthesized with (a) one, (b) two, and, (c) four 10 min continuous renebulization cycles. The frequency distributions were determined by examining the thicknesses and lateral sizes of over 200 QDs in the AFM images.

characterization under atomic force microscopy (AFM; Dimension Icon, Bruker Corp., Billerica, MA), high-resolution transmission electron microscopy (HRTEM; 200 kV accelerating voltage; Tecnai F20, FEI, Hillsboro, OR), X-ray diffraction (XRD; D8 Advance, Bruker Corp., Billerica, MA), and UV−vis absorption (Cary 60, Agilent Technologies, Santa Clara, CA), Raman (10 mW, 532 nm excitation, 200/2000 cm^{-1} acquisition range; Renishaw Oceania Pty. Ltd., Mulgrave, Victoria, Australia), and photoluminescence (PL; Fluoromax 4C, Horiba Scientific, Kyoto, Japan) spectroscopy. A minimum of 200 QDs were characterized with the AFM to obtain the thickness and lateral size distributions. The QD yield was calculated from the UV−vis absorption peaks using quinine sulfate (Sigma-Aldrich Pty. Ltd., Castle-Hill, New South Wales, Australia) as a calibration standard (see the Supporting Information, SI).

To briefly evaluate the quality of the QDs that were synthesized through an example application, we examine their activity as a catalyst for hydrogen evolution reactions (HERs). The MoS_2 QD catalysts were prepared by concentrating the sample in a desiccator after the exfoliation step and mixing them in ethanol and water in a 1:3 ratio together with 30 μL of Nafion (Sigma-Aldrich Pty. Ltd., Castle-Hill, New South Wales, Australia).[26] After sonication for 5 min, 10 μL of the suspension was deposited onto a 3 mm polished glassy carbon electrode, which was subsequently dried under room temperature. The electrochemical measurements were then conducted in 0.5 mL of H_2SO_4 in which a platinum wire was inserted as a counter electrode and Ag/AgCl was used as a reference electrode (see the SI). HER measurements were carried out using linear-sweep voltammetry (CHI1440, CH Instruments Inc., Austin, TX) without IR compensation across a potential range between −1.2 and +0.4 V at a scan rate of 10 mV/s at room temperature (see the SI).

Figure 2 shows the AFM images, thicknesses, and size distributions of the QDs produced over one, two, and four 10 min continuous renebulization cycles. It can be seen that the flakes become progressively thinner and smaller with increasing number of continuous renebulization cycles because the flakes from the previous cycle are successively cleaved laterally and simultaneously exfoliated to produce QDs, which are predominantly monolayer in thickness with a narrow lateral size distribution centered around a mean of approximately 8 nm, as confirmed from the HRTEM images in Figure S1. In addition, the HRTEM image also shows an 0.27 nm lattice spacing of a representative QD, which corresponds to the (100) lattice of MoS_2.[27]

Further confirmation is provided by the UV−vis, PL, XRD, and Raman spectra for the QDs obtained. The blue shift observed in the absorption spectra (Figure 3a) can be attributed to the quantum size effect (<50 nm) of the synthesized MoS_2 QDs,[28] whereas the two characteristic peaks at 230 and 280 nm can be ascribed to their excitonic

DOI: 10.1021/acsanm.8b00559
ACS Appl. Nano Mater. 2018, 1, 2503−2508

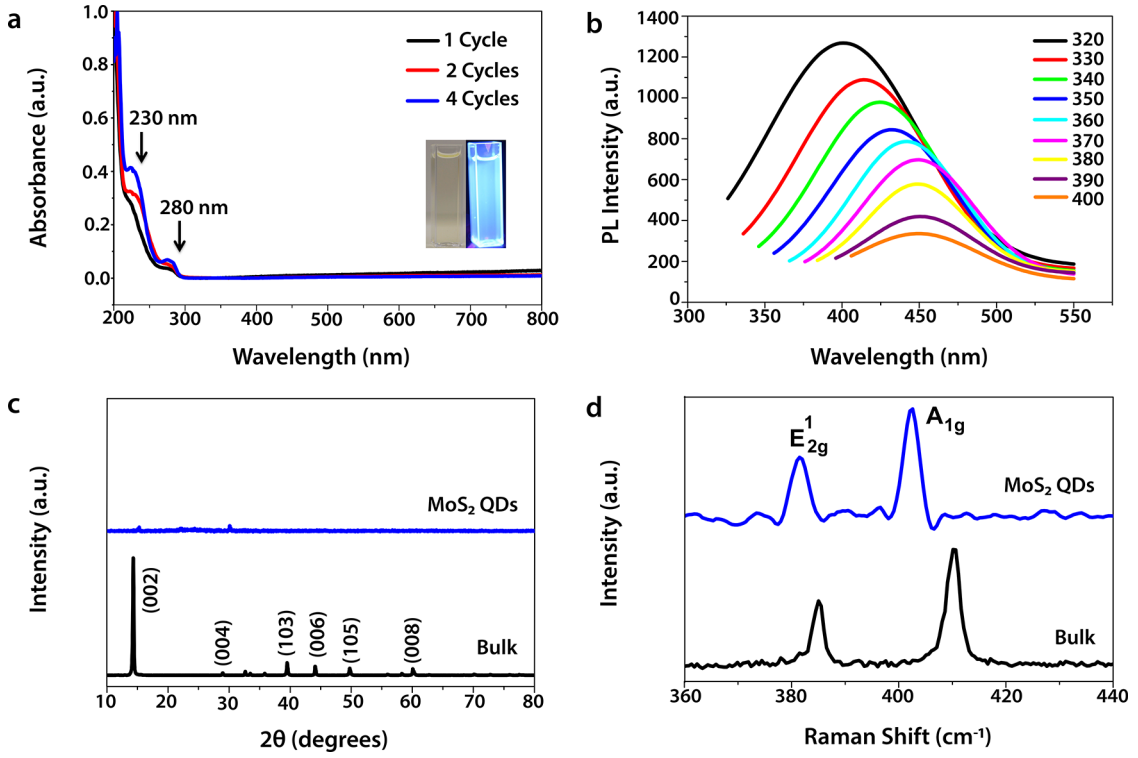

Figure 3. (a) UV−vis, (b) PL, (c) XRD, and (d) Raman spectra of the MoS_2 QDs obtained after four 10 min continuous renebulization cycles. The images in the inset of part a are of cuvettes containing the synthesized QDs under visible and UV (365 nm) illumination. Also shown in part a are the UV−vis absorbance spectra for the QDs obtained after one and two 10 min cycles. In parts c and d, the spectra associated with bulk MoS_2 are also presented.

features, consistent with that reported in the literature.[8,12,14,29] These appear to intensify with increasing number of continuous renebulization cycles as a consequence of the successive reduction in the lateral dimensions of the QDs. The excitation-dependent PL emission (Figure 3b), on the other hand, displays a red shift from 400 to 454 nm, which can be attributed to the *k* point in the Brillouin zone and the presence of many trap states similar to that detected in graphene QDs,[13,30] again consistent with that reported in the literature for MoS_2 QDs.[6,10,12]

The XRD spectra (Figure 3c) reveal a strong diffraction peak at $2\theta = 14.4°$ for bulk MoS_2, which can be ascribed to the (002) face of the crystals, and several small peaks at $2\theta = 29.0°$, 39.6°, 44.2°, 49.8°, and 60.2°, corresponding to the (004), (103), (006), (105), and (008) faces, respectively.[13] In contrast, it can be seen that the (002) peak has almost completely disappeared and that all of the other peaks are absent for the QDs synthesized over four 10 min continuous renebulization cycles, which is expected for materials that are thinned down to monolayers (Figure 2c), where there is little interference between the atomic planes associated with the *d* spacing of the crystal that gives rise to these diffraction peaks.[31] The appearance of a small peak at $2\theta = 28.4°$ corresponding to the (004) face of the crystal can be attributed to the restacking of MoS_2 QDs during the drying process.[31,32]

The Raman spectra in Figure 3d reveals two prominent peaks at approximately 382 and 402.6 cm^{-1}, corresponding to the E^1_{2g} in-plane mode (in which the Mo and S atoms vibrate in opposite directions) and the A_{1g} mode (S atoms vibrate out-of-plane), respectively. The wavenumber difference between the A_{1g} and E^1_{2g} modes can be seen to decrease from 25 cm^{-1} typical of bulk MoS_2 to approximately 20.6 cm^{-1} for the MoS_2 QDs, providing yet further confirmation that the exfoliated MoS_2 QDs predominantly consisted of single or double layers.[33]

Finally, it can be seen from Figure 4 and Table S1 that the QD production yield increases as the number of cycles

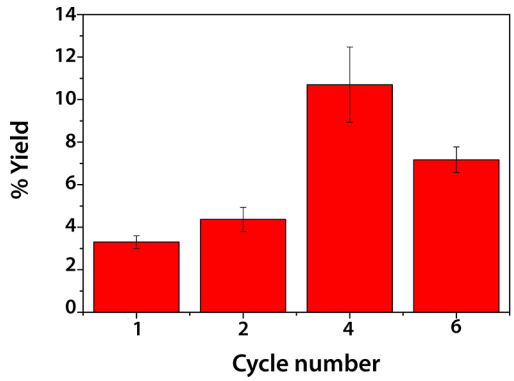

Figure 4. MoS_2 QD production yield after one, two, four, and six 10 min cycles. The error bars indicate the standard deviation in the yield measurements across triplicate runs.

increases, wherein a yield of approximately 10.7 ± 2%—much higher than the typical 2−3% QD yields[8,14] and a slight improvement above the highest value (9.65%)[17] reported in the literature to date (see Table S2 for a summary of the comparison)—was obtained in just 40 min, which is 2 orders of magnitude faster than conventional exfoliation processes. We note that increasing the number of renebulization cycles indefinitely does not result in further improvement of the yield. Instead, we observed that the yield over six cycles decreased to

DOI: 10.1021/acsanm.8b00559
ACS Appl. Nano Mater. 2018, 1, 2503−2508

7.2% possibly because of the precipitation of smaller QDs at the bottom of the Falcon tube, where they are not efficiently resuspended to the interface where they can be renebulized.

The electrochemical performance of the synthesized QDs as catalysts for HER is summarized in Table S3 as well as in Figure S2. It can be seen not only that the HER activity increases not just when MoS_2 QDs are used in place of its bulk counterpart but also that there is a progressive enhancement in the catalytic performance of the QDs synthesized with increasing number of continuous renebulization cycles, as seen from the successive decrease in the onset potential and Tafel slope with the addition of each 10 min cycle. This is likely because the QDs are subject to further lateral cleaving with increasing renebulization cycling, increasing the possibility for the introduction of more edge defects in the QDs, which are known to constitute active sites that enhance its catalytic activity.[34] We note, however, that enhancement in the HER activity ceases beyond four cycles, likely because no further reduction in the QD dimension was obtained with additional number of cycles to create more edge effects.

In summary, we have demonstrated the possibility of improving the exfoliation yield for the synthesis of MoS_2 QDs through a continuous renebulization process enabled by a miniature acoustomicrofluidic platform, without necessitating intercalating agents or high temperatures or pressures. Our results demonstrate that the desired QD characteristics, namely, the thinning of the QDs down to few-layer and single-layer thicknesses, uniformity in its lateral size distribution, and synthesis yield, improve with increasing number of continuous renebulization cycles. With just four cycles over a duration of 40 min, we obtain a yield of predominantly monolayer QDs with a 8.25 ± 4 nm mean lateral dimension of 10.7 ± 2%, which is significantly higher than the 2−3% yields obtained through conventional processes that typically take 2 orders of magnitude longer in processing times. The speed of the process then means that the production rate of 0.01 mg/min with a single device is already comparable with that afforded by conventional large-scale processes. Scalability toward higher throughput can further be enabled through parallelization with a large number of devices, given that each chipscale device is not only inexpensive to fabricate (typically ≈US$1) but also sufficiently miniaturized within a Falcon tube, which also allows for convenient subsequent downstream processing. We thus envisage the technology as an attractive alternative to conventional means for the industrial synthesis of TMD QDs for emerging applications in optoelectronics, photocatalysis, energy storage, and photonics or as transistors or biosensors, among other uses.

■ ASSOCIATED CONTENT

Supporting Information

The Supporting Information is available free of charge on the ACS Publications website at DOI: 10.1021/acsanm.8b00559.

TEM and HRTEM images of the MoS_2 QDs synthesized, MoS_2 QD yield, and HER measurements (PDF)

Movie of the experimental process (MOV)

■ AUTHOR INFORMATION

Corresponding Author

*E-mail: leslie.yeo@rmit.edu.au.

ORCID

Leslie Y. Yeo: 0000-0002-5949-9729

Notes

The authors declare no competing financial interest.

■ ACKNOWLEDGMENTS

S.M. is grateful to RMIT University for an Australian Postgraduate Award scholarship and acknowledges the help of Rhiannon Clark, Nafiseh Fahimi, and Anirban Paul with the yield and HER calculations. A.R.R. is grateful for an RMIT University Vice-Chancellor's Postdoctoral Fellowship and L.Y.Y. for an Australian Research Council (ARC) Future Fellowship (FT130100672). L.Y.Y. also acknowledges funding from the ARC through a Discovery Project grant (DP180102110). The authors thank the technicians associated with the RMIT Microscopy and Microanalysis Facility and MNRF for their help with the fabrication and characterization equipment used in the project.

■ REFERENCES

(1) Wang, Q. H.; Kalantar-Zadeh, K.; Kis, A.; Coleman, J. N.; Strano, M. S. Electronics and Optoelectronics of Two-Dimensional Transition Metal Dichalcogenides. *Nat. Nanotechnol.* **2012**, *7*, 699−712.

(2) Li, X.; Zhu, H. Two-Dimensional MoS_2: Properties, Preparation, and Applications. *J. Materiomics* **2015**, *1*, 33−44.

(3) Kuc, A.; Zibouche, N.; Heine, T. Influence of Quantum Confinement on the Electronic Structure of the Transition Metal Sulfide TS_2. *Phys. Rev. B: Condens. Matter Mater. Phys.* **2011**, *83*, 245213.

(4) Mak, K. F.; Shan, J. Photonics and Optoelectronics of 2D Semiconductor Transition Metal Dichalcogenides. *Nat. Photonics* **2016**, *10*, 216−226.

(5) Radisavljevic, B.; Radenovic, A.; Brivio, J.; Giacometti, i. V.; Kis, A. Single-Layer MoS_2 Transistors. *Nat. Nanotechnol.* **2011**, *6*, 147−150.

(6) Dong, H.; Tang, S.; Hao, Y.; Yu, H.; Dai, W.; Zhao, G.; Cao, Y.; Lu, H.; Zhang, X.; Ju, H. Fluorescent MoS_2 Quantum Dots:Ultrasonic Preparation, Up-Conversion and Down-Conversion Bioimaging, and Photodynamic Therapy. *ACS Appl. Mater. Interfaces* **2016**, *8*, 3107−3114.

(7) Gu, W.; Yan, Y.; Zhang, C.; Ding, C.; Xian, Y. One-Step Synthesis of Water-Soluble MoS_2 Quantum Dots via a Hydrothermal Method as a Fluorescent Probe for Hyaluronidase Detection. *ACS Appl. Mater. Interfaces* **2016**, *8*, 11272−11279.

(8) Fahimi-Kashani, N.; Rashti, A.; Hormozi-Nezhad, M. R.; Mahdavi, V. MoS_2 Quantum-Dots as a Label-Free Fluorescent Nanoprobe for the Highly Selective Detection of Methyl Parathion Pesticide. *Anal. Methods* **2017**, *9*, 716−723.

(9) Gopalakrishnan, D.; Damien, D.; Shaijumon, M. M. MoS_2 Quantum Dot-Interspersed Exfoliated MoS_2 Nanosheets. *ACS Nano* **2014**, *8*, 5297−5303.

(10) Ren, X.; Pang, L.; Zhang, Y.; Ren, X.; Fan, H.; Liu, S. F. One-Step Hydrothermal Synthesis of Monolayer MoS_2 Quantum Dots for Highly Efficient Electrocatalytic Hydrogen Evolution. *J. Mater. Chem. A* **2015**, *3*, 10693−10697.

(11) Li, B. L.; Chen, L. X.; Zou, H. L.; Lei, J. L.; Luo, H. Q.; Li, N. B. Electrochemically Induced Fenton Reaction of Few-Layer MoS_2 Nanosheets: Preparation of Luminescent Quantum Dots via a Transition of Nanoporous Morphology. *Nanoscale* **2014**, *6*, 9831−9838.

(12) Qiao, W.; Yan, S.; Song, X.; Zhang, X.; He, X.; Zhong, W.; Du, Y. Luminescent Monolayer MoS_2 Quantum Dots Produced by Multi-Exfoliation Based on Lithium Intercalation. *Appl. Surf. Sci.* **2015**, *359*, 130−136.

(13) Štengl, V.; Henych, J. Strongly Luminescent Monolayered MoS_2 Prepared by Effective Ultrasound Exfoliation. *Nanoscale* **2013**, *5*, 3387−3394.

DOI: 10.1021/acsanm.8b00559
ACS Appl. Nano Mater. 2018, 1, 2503−2508

(14) Wang, Y.; Ni, Y. Molybdenum Disulfide Quantum Dots as a Photoluminescence Sensing Platform for 2, 4, 6−Trinitrophenol Detection. *Anal. Chem.* **2014**, *86*, 7463−7470.
(15) Zhang, X.; Lai, Z.; Liu, Z.; Tan, C.; Huang, Y.; Li, B.; Zhao, M.; Xie, L.; Huang, W.; Zhang, H. A Facile and Universal Top-Down Method for Preparation of Monodisperse Transition-Metal Dichalcogenide Nanodots. *Angew. Chem., Int. Ed.* **2015**, *54*, 5425−5428.
(16) Wu, J.-Y.; Zhang, X.-Y.; Ma, X.-D.; Qiu, Y.-P.; Zhang, T. High Quantum-Yield Luminescent MoS_2 Quantum Dots with Variable Light Emission Created via Direct Ultrasonic Exfoliation of MoS_2 Nanosheets. *RSC Adv.* **2015**, *5*, 95178−95182.
(17) Dai, W.; Dong, H.; Fugetsu, B.; Cao, Y.; Lu, H.; Ma, X.; Zhang, X. Tunable Fabrication of Molybdenum Disulfide Quantum Dots for Intracellular MicroRNA Detection and Multiphoton Bioimaging. *Small* **2015**, *11*, 4158−4164.
(18) Wu, W.; Wang, L.; Li, Y.; Zhang, F.; Lin, L.; Niu, S.; Chenet, D.; Zhang, X.; Hao, Y.; Heinz, T. F.; Hone, J.; Wang, Z. L. Piezoelectricity of Single-Atomic-Layer MoS_2 for Energy Conversion and Piezotronics. *Nature* **2014**, *514*, 470−474.
(19) Ahmed, H.; Rezk, A.; Carey, B.; Wang, Y.; Mohiuddin, M.; Berean, K.; Russo, S.; Kalantar-zadeh, K.; Yeo, L. Ultrafast Acoustofluidic Exfoliation of Stratified Crystals. *Adv. Mater.* **2018**, *30*, 1704756.
(20) Friend, J.; Yeo, L. Y. Microscale Acoustofluidics: Microfluidics Driven via Acoustics and Ultrasonics. *Rev. Mod. Phys.* **2011**, *83*, 647.
(21) Ding, X.; Li, P.; Lin, S.-C. S.; Stratton, Z. S.; Nama, N.; Guo, F.; Slotcavage, D.; Mao, X.; Shi, J.; Costanzo, F.; Huang, T. J. Surface Acoustic Wave Microfluidics. *Lab Chip* **2013**, *13*, 3626−3649.
(22) Yeo, L. Y.; Friend, J. R. Surface Acoustic Wave Microfluidics. *Annu. Rev. Fluid Mech.* **2014**, *46*, 379−406.
(23) Destgeer, G.; Sung, H. J. Recent Advances in Microfluidic Actuation and Micro-Object Manipulation via Surface Acoustic Waves. *Lab Chip* **2015**, *15*, 2722−2738.
(24) Go, D. B.; Atashbar, M.; Ramshani, Z.; Chang, H.-C. Surface Acoustic Wave Devices for Chemical Sensing and Microfluidics: A Review and Perspective. *Anal. Methods* **2017**, *9*, 4112−4134.
(25) Qi, A.; Yeo, L. Y.; Friend, J. R. Interfacial Destabilization and Atomization Driven by Surface Acoustic Waves. *Phys. Fluids* **2008**, *20*, 074103.
(26) Zeng, X.; Niu, L.; Song, L.; Wang, X.; Shi, X.; Yan, J. Effect of Polymer Addition on the Structure and Hydrogen Evolution Reaction Property of Nanoflower-Like Molybdenum Disulfide. *Metals* **2015**, *5*, 1829−1844.
(27) Sweet, C.; Pramanik, A.; Jones, S.; Ray, P. C. Two-Photon Fluorescent Molybdenum Disulfide Dots for Targeted Prostate Cancer Imaging in the Biological II Window. *ACS Omega* **2017**, *2*, 1826−1835.
(28) Chikan, V.; Kelley, D. F. Size-Dependent Spectroscopy of MoS_2 Nanoclusters. *J. Phys. Chem. B* **2002**, *106*, 3794−3804.
(29) Xing, W.; Chen, Y.; Wang, X.; Lv, L.; Ouyang, X.; Ge, Z.; Huang, H. MoS_2 Quantum Dots with a Tunable Work Function for High-Performance Organic Solar Cells. *ACS Appl. Mater. Interfaces* **2016**, *8*, 26916−26923.
(30) Shinde, D. B.; Pillai, V. K. Electrochemical Preparation of Luminescent Graphene Quantum Dots from Multiwalled Carbon Nanotubes. *Chem. - Eur. J.* **2012**, *18*, 12522−12528.
(31) Xu, S.; Li, D.; Wu, P. One-Pot, Facile, and Versatile Synthesis of Monolayer MoS_2/WS_2 Quantum Dots as Bioimaging Probes and Efficient Electrocatalysts for Hydrogen Evolution Reaction. *Adv. Funct. Mater.* **2015**, *25*, 1127−1136.
(32) Li, B.; Jiang, L.; Li, X.; Ran, P.; Zuo, P.; Wang, A.; Qu, L.; Zhao, Y.; Cheng, Z.; Lu, Y. Preparation of Monolayer MoS_2 Quantum Dots Using Temporally Shaped Femtosecond Laser Ablation of Bulk MoS_2 Targets in Water. *Sci. Rep.* **2017**, *7*, 11182−11182.
(33) Li, H.; Zhang, Q.; Yap, C. C. R.; Tay, B. K.; Edwin, T. H. T.; Olivier, A.; Baillargeat, D. From Bulk to Monolayer MoS_2: Evolution of Raman Scattering. *Adv. Funct. Mater.* **2012**, *22*, 1385−1390.
(34) Yin, Y.; Han, J.; Zhang, Y.; Zhang, X.; Xu, P.; Yuan, Q.; Samad, L.; Wang, X.; Wang, Y.; Zhang, Z.; Zhang, P.; Cao, X.; Song, B.; Jin, S. Contributions of Phase, Sulfur Vacancies, and Edges to the Hydrogen Evolution Reaction Catalytic Activity of Porous Molybdenum Disulfide Nanosheets. *J. Am. Chem. Soc.* **2016**, *138*, 7965−7972.

DOI: 10.1021/acsanm.8b00559
ACS Appl. Nano Mater. 2018, 1, 2503−2508